Journal of Applied Research and Technology

www.jart.icat.unam.mx

Journal of Applied Research and Technology 21 (2023) 1042-1049

Original

Optimization with 2K factorial design in green synthesis of silver nanoparticles (AgNPs) using Porophyllum ruderale extract

J. N. Salgado-Delgado[a] • A. M. Salgado-Delgado[a] • R. Salgado-Delgado[a] • M. J. Granados-Baeza[a] • E. Rubio-Rosas[b] • A. Olarte-Paredes[a]*

[a]*Tecnológico Nacional de México/IT de Zacatepec, Calzada Tecnológico No. 27, C.P. 62780, Zacatepec de Hidalgo, Morelos. México, A.P. 45*
[b]*Facultad de Ingeniería Química, Benemérita Universidad Autónoma de Puebla, Av. San Claudio y 18 sur S/N edificio FIQ7 CU, San Manuel Puebla, Puebla C.P. 72570, México*

Received 09 06 2022; accepted 04 24 2023
Available 12 31 2023

Abstract: In recent years, metal nanoparticles are of scientific interest due to their properties, among which are optical, electrical, magnetic and high surface. In this work, a green, ecological and affordable synthesis of silver nanoparticles (AgNPs) using an alcoholic extract of *Porophyllum ruderale* leaves. The AgNPs obtained were characterized by IR spectroscopy to observe the formation of the carboxyl and rupture of hydroxyl that intervene in the synthesis mechanism. UV-Vis spectroscopy was used to study the surface plasmon band, confirming the peak absorbance wavelength at 385 nm. The morphological analysis by SEM showed AgNPs measuring 70–500 nm and spherical shapes. The optimal factors for AgNPs formation were found to be 100 °C temperature and 1:3 ratio. The work proved that by green synthesis using plant, metal ions such as Ag can be reduced and the AgNPs can be potentially applied as biosensors and antimicrobial agents, among others.

Keywords: Silver nanoparticles, plasmon, optimization, *Porophyllum ruderale*

*Corresponding author.
E-mail address: alfredo.op@zacatepec.tecnm.mx (Alfredo Olarte-Paredes).
Peer Review under the responsibility of Universidad Nacional Autónoma de México.

1. Introduction

Nanotechnology is a multidiscipline of great importance in scientific development (Ali et al., 2020), which has allowed for the synthesis of a wide variety of noble metal nanoparticles (MNPs). These MNPs show a high surface area (Echeverry-Chica et al., 2020) that considerably increases its ratio with surface/volume (Ali et al., 2018; Kumar et al., 2020). Particularly, MNPs of noble metals as silver, copper, and gold (Gómez-Garzón, 2018) are stable in oxidation and corrosion reactions; therefore, there is a surge in recent nanomaterial research since their novel properties are related to size, shape, and structure (Gangwar et al., 2021; Gomez-Garzón, 2018). Hu et al. (2021), they presented a green synthesis of AgNPs using Rhodiola rosea rhizome extract and studied antioxidant activity, during the synthesis they observed that the color of the solution changed from green to brown-gray, which confirmed the formation of AgNPs. Similarly, they observed the peak of the SPR at 437 nm and the transmission electron microscopy (TEM) study evidenced that the AgNPs measured 10 nm approximately and were spherical (Hu et al., 2021).

It is known that AgNPs are semicrystalline structures with several properties, such as electrical conductivity, antimicrobial activity, enzymatic activity, and optical activity (Cuervo-Osorio et al., 2020; Wang & Wei, 2022). The SPR is present in the visible region of an electromagnetic spectrum (Hu et al., 2021); this phenomenon occurs when the particles are smaller than the wavelength of incident light (Hu et al., 2021; Rathnakumar et al., 2021). When AgNPs are irradiated with light, the surface electrons are excited, so their energy rises (Biswas & Mulaba-Bafubiandi, 2016), increasing the energy level of the electrons (conduction band) (Biswas & Mulaba-Bafubiandi, 2016; Höglund et al., 2021) and producing a delocalized oscillation of the electrons confined on the surface (polariton) (Biswas & Mulaba-Bafubiandi, 2016; Kumar et al., 2020) of surface plasmon. The polariton is a quasiparticle created by a photon coupled to an electric dipole (Sachan et al., 2014). In particles < 30 nm a dipole (Osorio Anaya et al., 2019) is produced and quadrupoles and/or multipoles are generated in particles > 30 nm (Pu et al., 2018). This is observed in the variation of the wavelength in the visible region, directly proportional to the size of the AgNPs (Osorio Anaya et al., 2019).

Currently, there are different methods to synthesize MNPs; they are classified as top-down, the physical method that reduces aggregation size to nanometers, and bottom-up (Abid et al., 2022), the chemical method that starts from molecular dispersion to a nanometric size. The latter is the simplest and most used. It provides control on the particle size but is costly and highly polluting, producing toxic effects in the environment (Chandra & Singh, 2018; Mirajkar et al., 2021; Upadhyay et al., 2019). On the other hand, green synthesis is no need for high pressures, high energy, and toxic chemicals, its low cost and friendly to the environment (Kumar et al., 2021; Saif et al., 2016; Santos-Espinoza et al., 2020). Plants contain metabolites and biochemical substances (Patiño-Ruiz et al., 2021) that can be stabilizing and reducing agents in MNPs synthesis (Balbuena et al., 2020). There is a large number of hydroxyl groups (-OH) in Porophyllum ruderale, which confers high stability to the radical after MNPs synthesis (Balbuena et al., 2020) since the -OH groups are in ortho position (Fukalova et al., 2022). Therefore, in the present work, a green synthesis of AgNPs using an alcoholic extract Porophyllum ruderale (P. ruderale) leaves, which contains a high phenolic compounds (Singh et al., 2020) that play a key role in particle stabilization, bio-reduction and bio-capping (Fukalova et al., 2022). They also reduce Ag^{+} and Ag^{0} ions, creating zero-valent particles that act as nucleation sites due to the presence of -OH groups (Danish et al., 2021). These AgNPs have relatively low toxicity which promising antimicrobial agent, antiviral, and biocide (Raman et al., 2021).

2. Materials and methods

2.1. Materials

Silver nitrate ($AgNO_3$) Merck (Darmstadt, CA: 7761-88-8, Germany), Ethanol Merck (Darmstadt, CAS: 64-17-5, Germany), distilled water (Químicos Farmacéuticos Industriales SA de CV). *P. ruderale* was collected in Morelos, Mexico.

2.2. Porophyllum ruderale extraction

Fresh *P. ruderale* leaves were macerated to extract *P. ruderale* since they have the highest phenolic compound content. The leaves were cut, weighed (20 g), and washed with distilled water to eliminate dust impurities (Sameen et al., 2014). They were placed in a mortar for maceration, and an 80% ethanol solution was added, maintaining a solvent/leaves ratio of 2:1 (v/w). The macerated solution was placed in a 100-mL Erlenmeyer flask, which was capped with a rubber stopper, maintaining an extraction time of 36 h. The solution was then filtered and placed in vials kept at 4°C until use (Fukalova et al., 2022).

2.3. Green synthesis of AgNPs extract of P. ruderale

The experimental design for the AgNPs was done considering two factors: synthesis temperature (80, 90, and 100 °C), ratio (1:2 and 1:3 v/v) of [reducing agent (extract:RA)]: [precursor agent ($AgNO_3$ 0.1M:PA)]. Six samples with replicates were obtained, as shown in Table 1.

The AgNPs were synthesized by green synthesis, using silver nitrate (0.1 M $AgNO_3$) as precursor agent and P. ruderale extract as reducing agent. The temperature of the extract was set at one of the temperatures in the experimental design and $AgNO_3$ was added in a constant drip to prevent particle agglomeration. The temperature must be controlled, and the

mix kept under constant magnetic stirring to prevent fluctuation and AgNPs oxidation. Once the solution turns brown, stirring is stopped and the mix is left to cool until it reaches room temperature (25 °C). The flask is covered with foil for AgNPs stability (Kumar et al., 2020).

Table 1. Experimental design of AgNPs (P: extract).

No.	SAMPLE	TEMPERATURE °C	RA:PA
1	1:2P80	80	1:2
2	1:2P90	90	1:2
3	1:2P100	100	1:2
4	1:3P80	80	1:3
5	1:3P90	90	1:3
6	1:3P100	100	1:3

Figure 1 shows the reaction mechanism of the AgNPs synthesis. As stated above, contains phenolic compounds that are key to the synthesis and stability of MNPs (Patel et al., 2021). The reduction of Ag^{+} ions into Ag^{0} are carried out from -OH groups, transferring hydrogen atoms for the neutralization of free radicals, creating a coordinate Ag–O complex and the C=O (carbonyl) group. As the number of functional hydroxyl groups is higher and in ortho position, the particles are more stable due to electron delocalization (Basiuk& Basiuk, 2015).

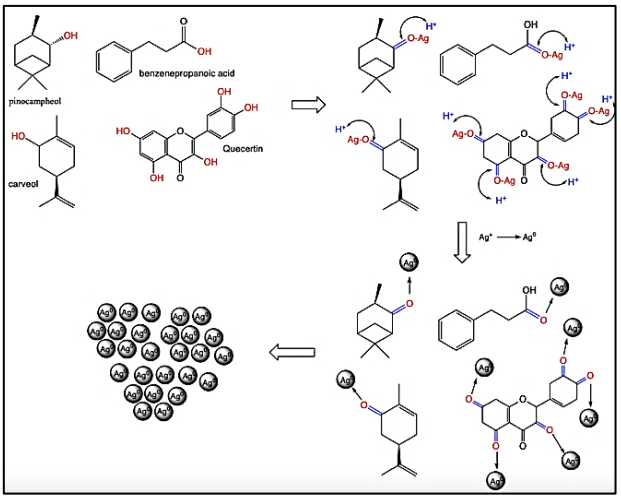

Figure 1. Synthesis mechanism of AgNPs.

2.4. Optimization design

A 2^{k} experimental design in which the parameters temperature and extract/$AgNO_3$ ratio were evaluated was used; particle size was maintained as the output variable. In the experiment, six samples with replicates were obtained to reach a total of 12 sample data. An optimization analysis was done using the parameters above and the optimal conditions for the experiment were identified.

2.5. Characterization

The AgNPs where characterized through Fourier transform infrared spectroscopy (FTIR) using a Perkin Elmer Spectrum Two FTIR spectrometer in the spectrum range 4000–500 cm^{-1} to observe the functional groups and characteristic bands of AgNPs. The morphological analysis and particle size were identified through scanning electron microscopy (SEM) in a JEOL microscope (JSM 6010A, Musashino, Akishima, Tokyo 196-8558, Japan) in SEI mode and 15 kV with a metallic coating (gold). The UV-visible analysis was done in a UV-Vis spectrophotometer (Velab Model VE-5600UV, Mexico) to identify the surface plasmon of AgNPs.

3. Results

In this work, AgNPs were obtained through green synthesis from *P. ruderale*, as stated before, and Ag ions were reduced by the phenolic compounds in the plant as the author Patel et al. (2021) mention (Balbuena et al., 2020; Sánchez et al., 2018). Figure 2 shows the AgNPs samples: The $AgNO^{3}$ solution is colorless while the extract shows a green color; when the reaction takes place, the solution turns dark brown, the first indication that AgNPs are formed. Cruz et al. (2012) report that the changes in color shows AgNPs attributed to the interaction of the metal conduction electrons in the nanoparticles with incident photons (Blakney et al., 2019; Sankar et al., 2013).

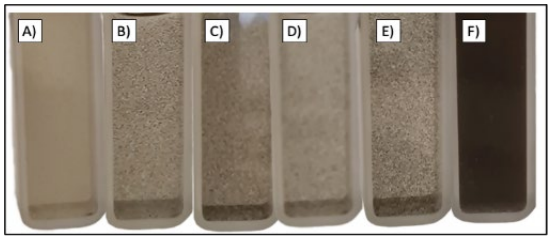

Figure 2. Silver nanoparticles (A) 1:2P80, (B) 1:2P90, (C)1:2P100, (D) 1:3P80, (E) 1:3P90, and (F) 1:3P100.

3.1. Fourier transform infrared spectroscopy (FTIR)

Figure 3 shows the FTIR spectra of *P. ruderale* with the following conditions: 1:2P80, 1:2P90, and 1:2P100 in the wavenumber range 4000–500 cm^{-1} and 16 scans. The 1:2 sample (at different temperatures) shows the signals at 3400, 1402 and 1045 cm^{-1} (stretching of the O-H groups, O-H in-plane bending and C-O stretching, respectively); these signals are reduced as the temperature increases, since the -OH groups dissociate during synthesis creating a coordinate complex as mention Akintelu et al. (2020); that is, a compound consisting of a central ion (Ag) with free orbitals to accept electrons and form a ligand with oxygen (Akintelu et al., 2020; Cruz et al., 2012), creating carbonyl groups (C=O stretching at 1650 cm^{-1}). This has been previously discussed in 2020 with the authors

Adelware et al. 2020 referring to hydrogen transference during free-radical neutralization in the synthesis of AgNPs (Adelware et al., 2020) (see process in Figure 1).

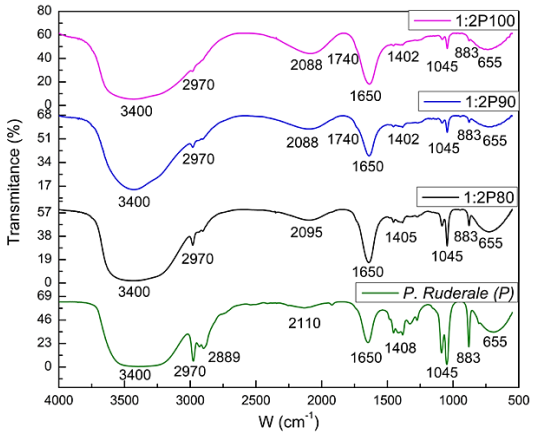

Figure 3. Spectra in the range 4000–500 cm^{-1}; *P. ruderale* samples and 1:2P (80 °C, 90 °C, and 100 °C).

Figure 4 shows the FTIR spectra of *P. ruderale* with the following conditions: 1:3P80, 1:3P90, and 1:3P100 in the wavenumber range 4000–500 cm^{-1} and 16 scans. At 3401 cm^{-1} the stretching of the -OH extract and water is observed. The symmetric and asymmetric stretching of the aliphatic structure C-H is found at 2970–2889 cm^{-1}. The stretching of the carbonyl group (C=O) is found at 1650 cm^{-1}. The CH_2 and CH_3 aliphatic flexion occurs at 1400-1500 cm^{-1}. In-plane bending of the -OH groups is observed at 1402 cm^{-1}. The stretching of C-O in the extract is found at 1045 cm^{-1} and the out-of-plane bending of -OH is observed at 660 cm^{-1}.

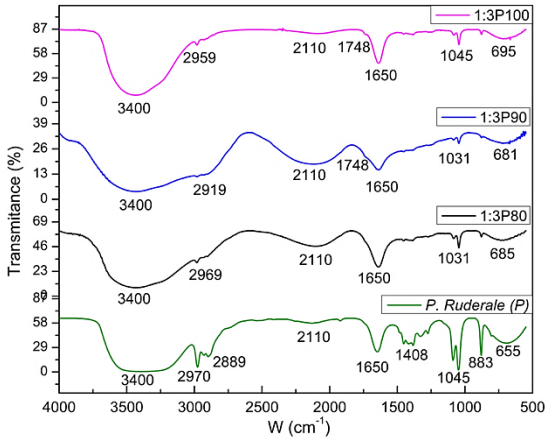

Figure 4. Spectra in the range 4000–500 cm^{-1}; *P. ruderale* samples and 1:3P (80 °C, 90 °C, and 100 °C).

3.2. UV-Vis spectroscopy

The UV-Vis analysis of AgNPs shows an intense absorption peak due to surface plasmon excitation related by size, shape, and interactions of AgNPs (Cobos et al., 2019). The plasmon band was found in a range between 379 and 389 nm (Figure 5), produced because the valence and conduction bands are very close to each other. This promotes the oscillation of the free electrons in AgNPs with the light wave (Roy et al., 2019). The AgNPs mainly show unique spectral responses with specific wavelengths between 350 and 500 nm. Roy et al. (2019) reported that the spherical SPR was observed between 370 and 480 nm.

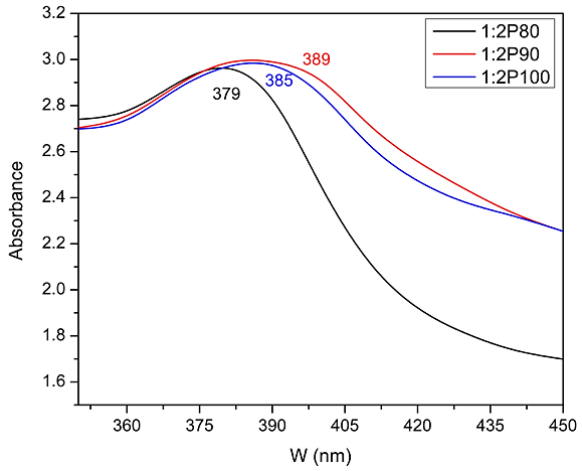

Figure 5. UV-Vis spectroscopy of AgNPs of 1 :2P (80 °C, 90 °C, and 100 °C).

Figure 6 shows the spectra of samples 1:3P (80 °C, 90 °C, and 100 °C) in the range 350–450 nm. There is a peak absorption in the wavelength of 360 nm at 100 °C, 370 nm at 80 °C, and 390 nm at 90 °C. A wide curve indicates a difference between the particle size, as observed in 1:3P90: The curve is wide and the size ranges from 100 to 200 nm. Still, the SPR of AgNPs is found between 380 and 430 nm with a defined structure that is spherical as reported by Roy et al. 2019, Gaikwad et al., 2006 and Zhao et al. 2010. Sun & Xia (2003) mention that for absorption wavelengths over 500 nm there are nanorod-like structures and thus the UV-Vis results in this study can predict the spherical geometry and a size distribution depending on the working temperature (Noguez, 2007).

3.3. Morphological analysis by SEM

In the morphological analysis (SEM) of the AgNPs, the NPs measured 70–500 nm and showed a spherical shape. The size can vary due to the factors previously mentioned: temperature (Roy et al., 2019) and extract-$AgNO_3$ ratio. Figure 7 shows the

SEM micrographs of the 1:2 and 1:3 ratio for the different working temperatures (80 °C and 100 °C). It is observed that there is an agglomeration of AgNPs due to the Van der Waals forces that are generated because of the affinity between AgNPs that could modify the surface tension of AgNPs.

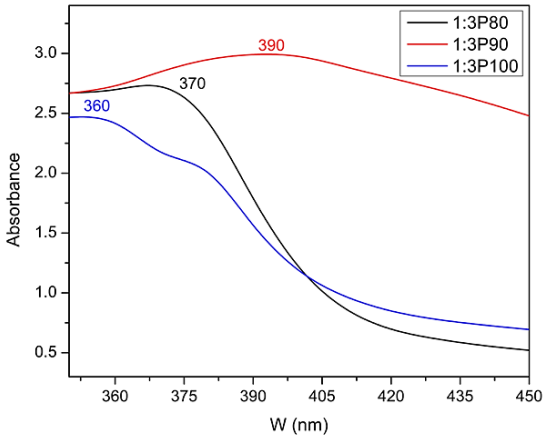

Figure 6. UV-Vis spectroscopy of AgNPs of 1:3P (80 °C, 90 °C, and 100 °C).

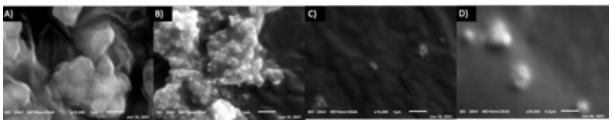

Figure 7. Micrographs A) 1:2P80 15000x, B) 1:2P100 15000x, C) 1:3P80 15000x, D) 1:3P100 30000x.

Figure 8 shows the micrographs of the 1:2P90 (Figure 7A) and 1:3P90 (Figure 7C) samples with their histograms, with the help of the ImageJ software, the diameters of the particles were measured and it is observed that they have an approximate size of (Figure 7B) 60 nm to 200 nm and when the ratio change also the diameter too with 50 nm to 130 nm (Figure 7D), being the 1:3P90 sample that presented the best result of smaller nanometric size.

3.4. Optimization of silver nanoparticles

A 2^k (k = 2) experimental design was established for AgNPs optimization. The analysis used temperature with three levels (80 °C, 90 °C, and 100 °C) as variable and the ratio RA:PA with two levels (1:2 and 1:3) (Blakney et al., 2019; Kauffman et al., 2015; Sankar et al., 2013). The response variable measured was the particle size (Sun & Xia, 2003). Cuervo-Osorio et al. (2020), carried out an optimization of AgNPs where they showed that the temperature influences the size of the particle. The factors affect the particle size, establishing that the optimal factors are T=100 °C and an RA:PA ratio (1:3) (see Figure 9).

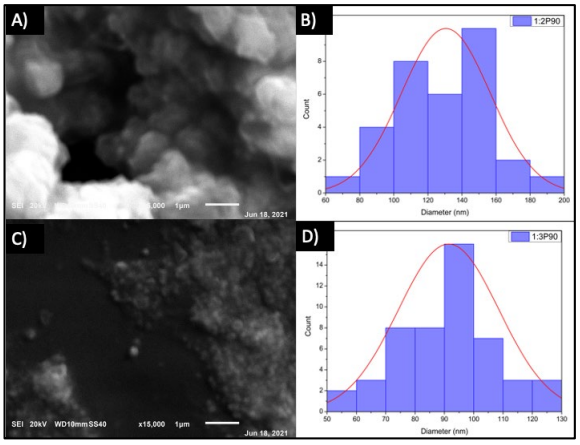

Figure 8. A) Micrographs 1:2P90 15000x, B) Histogram 1:2P90, C) Micrographs 1:3P90 15000x, D) Histogram 1:3P90.

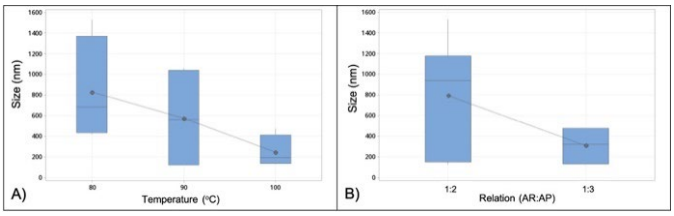

Figure 9. Optimization analysis of variables A) temperature and B) RA:PA ratio.

4. Conclusion

In this work, the green synthesis of AgNPs using *P. ruderale* extract was described. It was demonstrated that the synthesis is possible from vegetable extracts without producing toxic agents into the environment during the process. During the nanoparticle obtainment process, the change from green to brown color was observed, which confirmed the presence of AgNPs (Saha et al., 2021). The FTIR analysis proves that the hydroxyl groups (-OH) are the main functional groups for the synthesis, reducing Ag^+ ions and stabilizing AgNPs. The UV-Vis analysis identifies the plasmon band characteristic of the AgNPs, and it is observed at 385 nm (specific range of the AgNPs and with nanospherical shape SPR mode), as confirmed by morphological analysis (SEM), in which AgNPs with sizes from 70 nm to 500 nm were observed with a defined spherical shape. The optimization analysis demonstrates that the temperature of 100 °C is the most optimal factor for the generation of AgNPs and a 1:3 ratio of RA:PA. The results are promising for applications in nanomaterials, and together with the inherent properties of AgNPs, it can be used in different areas as a biocide, antimicrobial materials, and biosensors, among others.

Conflict of interest

The authors have no conflict of interest to declare.

Funding

The authors received no specific funding for this work.

References

Ali, K. A., Yao, R., Wu, W., Masum, M. M. I., Luo, J., Wang, Y., ... & Li, B. (2020). Biosynthesis of silver nanoparticle from pomelo (Citrus Maxima) and their antibacterial activity against acidovorax oryzae RS-2. *Materials Research Express*, *7*(1), 015097.
https://doi.org/10.1088/2053-1591/ab6c5e

Abid, N., Khan, A. M., Shujait, S., Chaudhary, K., Ikram, M., Imran, M., ... & Maqbool, M. (2022). Synthesis of nanomaterials using various top-down and bottom-up approaches, influencing factors, advantages, and disadvantages: A review. *Advances in Colloid and Interface Science*, *300*, 102597.
https://doi.org/10.1016/j.cis.2021.102597

Adewale, O. B., Egbeyemi, K. A., Onwuelu, J. O., Potts-Johnson, S. S., Anadozie, S. O., Fadaka, A. O., ... & Onasanya, A. (2020). Biological synthesis of gold and silver nanoparticles using leaf extracts of Crassocephalum rubens and their comparative in vitro antioxidant activities. *Heliyon*, *6*(11).
https://doi.org/10.1016/j.heliyon.2020.e05501

Akintelu, S. A., Bo, Y., & Folorunso, A. S. (2020). A review on synthesis, optimization, mechanism, characterization, and antibacterial application of silver nanoparticles synthesized from plants. *Journal of Chemistry*, *2020*, 1-12.
https://doi.org/10.1155/2020/3189043

Ali, J. A., Kolo, K., Manshad, A. K., & Mohammadi, A. H. (2018). Recent advances in application of nanotechnology in chemical enhanced oil recovery: Effects of nanoparticles on wettability alteration, interfacial tension reduction, and flooding. *Egyptian journal of petroleum*, *27*(4), 1371-1383.
https://doi.org/10.1016/j.ejpe.2018.09.006

Basiuk, V. A., & Basiuk, E. V. (2015). Green processes for nanotechnology. *Springer*, 446.
https://doi.org/10.1007/978-3-319-15461-9

Biswas, S., & Mulaba-Bafubiandi, A. F. (2016). Optimization of process variables for the biosynthesis of silver nanoparticles by Aspergillus wentii using statistical experimental design. *Advances in Natural Sciences: Nanoscience and Nanotechnology*, 7(4).
https://doi.org/10.1088/2043-6262/7/4/045005

Blakney, A. K., McKay, P. F., Ibarzo Yus, B., Hunter, J. E., Dex, E. A., & Shattock, R. J. (2019). The skin you are in: design-of-experiments optimization of lipid nanoparticle self-amplifying RNA formulations in human skin explants. *ACS nano*, *13*(5), 5920-5930.
https://doi.org/10.1021/acsnano.9b01774

Chandra, A., & Singh, M. (2018). Biosynthesis of amino acid functionalized silver nanoparticles for potential catalytic and oxygen sensing applications. *Inorganic Chemistry Frontiers*, *5*(1), 233-257.
https://doi.org/10.1039/c7qi00569e

Cobos, M., De-La-Pinta, I., Quindós, G., Fernández, M. J., & Fernández, M. D. (2019). One-step eco-friendly synthesized silver-graphene oxide/poly (vinyl alcohol) antibacterial nanocomposites. *Carbon*, *150*, 101-116.
https://doi.org/10.1016/j.carbon.2019.05.011

Cruz, D. A., Rodríguez, M. C., López, J. M., Herrera, V. M., Orive, A. G., & Creus, A. H. (2012). Nanopartículas metálicas y plasmones de superficie: una relación profunda. Avances en Ciencias e Ingeniería, 3(2), 67-78.

Cuervo-Osorio, G. A., Escobar-Jaramillo, M., & Ossa-Orozco, C. P. (2020). Diseño factorial 2k para la optimización de la síntesis de nanopartículas de plata para su aplicación en biomateriales. *Revista ION*, *33*(1), 17-32.
https://doi.org/10.18273/revion.v33n1-2020002

Danish, M., Altaf, M., Robab, M. I., Shahid, M., Manoharadas, S., Hussain, S. A., & Shaikh, H. (2021). Green synthesized silver nanoparticles mitigate biotic stress induced by Meloidogyne incognita in Trachyspermum ammi (L.) by improving growth, biochemical, and antioxidant enzyme activities. *ACS omega*, *6*(17), 11389-11403.
https://doi.org/10.1021/acsomega.1c00375

Echeverry-Chica, J., Naranjo-Díaz, A., & Araque-Marín, P. (2020). Nanopartículas de plata funcionalizadas in situ con D-limoneno: efecto en la actividad antibacteriana. *Revista Ion*, *33*(1), 79-92.
https://doi.org/10.18273/revion.v33n1-2020008

Fukalova Fukalova, T., García-Martínez, M. D., & Raigón, M. D. (2022). Nutritional composition, bioactive compounds, and volatiles profile characterization of two edible undervalued plants: Portulaca oleracea L. and Porophyllum ruderale (Jacq.) Cass. *Plants*, *11*(3), 377.
https://doi.org/10.3390/plants11030377

Gaikwad, A. V., Verschuren, P., Eiser, E., & Rothenberg, G. (2006). A simple method for measuring the size of metal nanoclusters in solution. *The Journal of Physical Chemistry B*, *110*(35), 17437-17443.
https://doi.org/10.1021/jp063644n

Gangwar, C., Yaseen, B., Kumar, I., Singh, N. K., & Naik, R. M. (2021). Growth kinetic study of tannic acid mediated monodispersed silver nanoparticles synthesized by chemical reduction method and its characterization. *ACS omega*, *6*(34), 22344-22356.
https://doi.org/10.1021/acsomega.1c03100

Gómez-Garzón, M. (2018). Nanomateriales, nanopartículas y síntesis verde. *Revista Repertorio de Medicina y Cirugía*, *27*(2).
https://doi.org/10.31260/RepertMedCir.v27.n2.2018.191

Höglund, M., Garemark, J., Nero, M., Willhammar, T., Popov, S., & Berglund, L. A. (2021). Facile processing of transparent wood nanocomposites with structural color from plasmonic nanoparticles. *Chemistry of Materials*, *33*(10), 3736-3745.
https://doi.org/10.1021/acs.chemmater.1c00806

Hu, D., Yang, X., Chen, W., Feng, Z., Hu, C., Yan, F., ... & Chen, Z. (2021). Rhodiola rosea rhizome extract-mediated green synthesis of silver nanoparticles and evaluation of their potential antioxidant and catalytic reduction activities. *ACS omega*, *6*(38), 24450-24461.
https://doi.org/10.1021/acsomega.1c02843

Kauffman, K. J., Dorkin, J. R., Yang, J. H., Heartlein, M. W., DeRosa, F., Mir, F. F., ... & Anderson, D. G. (2015). Optimization of lipid nanoparticle formulations for mRNA delivery in vivo with fractional factorial and definitive screening designs. *Nano letters*, *15*(11), 7300-7306.
https://doi.org/10.1021/acs.nanolett.5b02497

Kumar, H., Bhardwaj, K., Kuča, K., Kalia, A., Nepovimova, E., Verma, R., & Kumar, D. (2020). Flower-based green synthesis of metallic nanoparticles: Applications beyond fragrance. *Nanomaterials*, *10*(4), 766.
https://doi.org/10.3390/nano10040766

Balbuena, L. M., Vivas, B. M. C., López, I. S., Lino, A. C., & García, J. C. R. (2020). Antioxidantes naturales y su poder reductor frente a iones plata: alternativa en la recuperación de metales. *CIBA Revista Iberoamericana de las Ciencias Biológicas y Agropecuarias*, *9*(17), 1-22.
https://doi.org/10.23913/ciba.v9i17.95

Mirajkar, S., Rathod, P., Pawar, B., Penna, S., & Dalvi, S. (2021). γ-Irradiated chitosan mediates enhanced synthesis and antimicrobial properties of chitosan–silver (Ag) nanocomposites. *ACS omega*, *6*(50), 34812-34822.
https://doi.org/10.1021/acsomega.1c05358

Noguez, C. (2007). Surface plasmons on metal nanoparticles: the influence of shape and physical environment. *The Journal of Physical Chemistry C*, *111*(10), 3806-3819.
https://doi.org/10.1021/jp066539m

Osorio Anaya, A. M., Manrique Fajardo, J. J., & Cornejo Sánchez, Ó. (2019). Estudio teórico del plasmón en nanoesferas de oro. *Revista de la Sociedad Química del Perú*, *85*(4), 432-439.
https://doi.org/10.37761/rsqp.v85i4.257

Patel, A., Enman, J., Gulkova, A., Guntoro, P. I., Dutkiewicz, A., Ghorbani, Y., ... & Matsakas, L. (2021). Integrating biometallurgical recovery of metals with biogenic synthesis of nanoparticles. *Chemosphere*, *263*, 128306.
https://doi.org/10.1016/j.chemosphere.2020.128306

Patiño-Ruiz, D. A., Meramo-Hurtado, S. I., González-Delgado, A. D., & Herrera, A. (2021). Environmental sustainability evaluation of iron oxide nanoparticles synthesized via green synthesis and the coprecipitation method: A comparative life cycle assessment study. *ACS omega*, *6*(19), 12410-12423.
https://doi.org/10.1021/acsomega.0c05246

Pu, F., Huang, Y., Yang, Z., Qiu, H., & Ren, J. (2018). Nucleotide-based assemblies for green synthesis of silver nanoparticles with controlled localized surface plasmon resonances and their applications. *ACS Applied Materials & Interfaces*, *10*(12), 9929-9937.
https://doi.org/10.1021/acsami.7b18915

Raman, N., Sudharsan, S., Veerakumar, V., Pravin, N., & Vithiya, K. (2012). Pithecellobium dulce mediated extra-cellular green synthesis of larvicidal silver nanoparticles. *Spectrochimica Acta Part A: Molecular and Biomolecular Spectroscopy*, *96*, 1031-1037.
https://doi.org/10.1016/j.saa.2012.08.011

Rathnakumar, S., Bhaskar, S., Rai, A., Saikumar, D. V., Kambhampati, N. S. V., Sivaramakrishnan, V., & Ramamurthy, S. S. (2021). Plasmon-coupled silver nanoparticles for mobile phone-based attomolar sensing of Mercury ions. *ACS Applied Nano Materials*, *4*(8), 8066-8080. https://doi.org/10.1021/acsanm.1c01347

Roy, A., Bulut, O., Some, S., Mandal, A. K., & Yilmaz, M. D. (2019). Green synthesis of silver nanoparticles: biomolecule-nanoparticle organizations targeting antimicrobial activity. *RSC advances*, *9*(5), 2673-2702. https://doi.org/10.1039/c8ra08982e

Sachan, R., Malasi, A., Ge, J., Yadavali, S., Krishna, H., Gangopadhyay, A., ... & Kalyanaraman, R. (2014). Ferroplasmons: intense localized surface plasmons in metal-ferromagnetic nanoparticles. *ACS nano*, *8*(10), 9790-9798. https://doi.org/10.1021/nn5031719

Saha, P., Mahiuddin, M., Islam, A. N., & Ochiai, B. (2021). Biogenic synthesis and catalytic efficacy of silver nanoparticles based on peel extracts of citrus macroptera fruit. *ACS omega*, *6*(28), 18260-18268. https://doi.org/10.1021/acsomega.1c02149

Saif, S., Tahir, A., & Chen, Y. (2016). Green synthesis of iron nanoparticles and their environmental applications and implications. *Nanomaterials*, *6*(11), 209. https://doi.org/10.3390/nano6110209

Sameen, A., Fathima, S. J., Ramlal, S., Kumar, S., & Khanum, F. (2014). Nanopackaging of silver using spice extract and their characterization. *Science, Technology and Arts Research Journal*, *3*(3), 52-56. https://doi.org/10.4314/star.v3i3.9

Sánchez, Y., García-Quintero, A., & Palencia, M. (2018). Determination and distribution of size of inorganic particles by spectral deconvolution of surface plasmon resonance. *Journal of Science with Technological Applications*, 5, 45-54. https://doi.org/10.34294/j.jsta.18.5.34

Sankar, R., Karthik, A., Prabu, A., Karthik, S., Shivashangari, K. S., & Ravikumar, V. (2013). Origanum vulgare mediated biosynthesis of silver nanoparticles for its antibacterial and anticancer activity. *Colloids and Surfaces B: Biointerfaces*, *108*, 80-84. https://doi.org/10.1016/j.colsurfb.2013.02.033

Santos-Espinoza, A., Gutiérrez-Miceli, F., Ruíz-Valdiviezo, V., & Montes-Molina, J. (2020). El papel de los compuestos polifenólicos en la síntesis verde de nanopartículas metálicas. BioTecnología, 24(2), 46-46.

Singh, A., Gautam, P. K., Verma, A., Singh, V., Shivapriya, P. M., Shivalkar, S., ... & Samanta, S. K. (2020). Green synthesis of metallic nanoparticles as effective alternatives to treat antibiotics resistant bacterial infections: A review. *Biotechnology Reports*, *25*, e00427. https://doi.org/10.1016/j.btre.2020.e00427

Sun, Y., & Xia, Y. (2003). Gold and silver nanoparticles: a class of chromophores with colors tunable in the range from 400 to 750 nm. *Analyst*, *128*(6), 686-691. https://doi.org/10.1039/B212437H

Upadhyay, P., Mishra, S. K., Purohit, S., Dubey, G. P., Singh Chauhan, B., & Srikrishna, S. (2019). Antioxidant, antimicrobial and cytotoxic potential of silver nanoparticles synthesized using flavonoid rich alcoholic leaves extract of Reinwardtia indica. *Drug and chemical toxicology*, *42*(1), 65-75. https://doi.org/10.1080/01480545.2018.1488859

Wang, Y., & Wei, S. (2021). Green fabrication of bioactive silver nanoparticles using Mentha pulegium extract under alkaline: An enhanced anticancer activity. *ACS omega*, *7*(1), 1494-1504. https://doi.org/10.1021/acsomega.1c06267

Zhao, T., Sun, R., Yu, S., Zhang, Z., Zhou, L., Huang, H., & Du, R. (2010). Size-controlled preparation of silver nanoparticles by a modified polyol method. *Colloids and Surfaces A: Physicochemical and Engineering Aspects*, *366*(1-3), 197-202. https://doi.org/10.1016/j.colsurfa.2010.06.005